

Received January 20, 2022, accepted February 3, 2022, date of publication February 7, 2022, date of current version February 15, 2022.

Digital Object Identifier 10.1109/ACCESS.2022.3149755

On the Fractionalization of the Shift Operator on Graphs

GUILHERME B. RIBEIRO¹, JOSÉ R. DE OLIVEIRA NETO^{1,2}, (Member, IEEE),
AND JULIANO B. LIMA¹, (Senior Member, IEEE)

¹Department of Electronics and Systems, Federal University of Pernambuco, Recife 50740-550, Brazil

²Department of Mechanical Engineering, Federal University of Pernambuco, Recife 50740-550, Brazil

Corresponding author: Juliano B. Lima (juliano_bandeira@ieee.org)

This work was supported in part by the Conselho Nacional de Desenvolvimento Científico e Tecnológico (CNPq) under Grant 310142/2020-2 and Grant 409543/2018-7, and in part by the Coordenação de Aperfeiçoamento de Pessoal de Nível Superior (CAPES).

ABSTRACT The theory of graph signal processing has been established with the purpose of generalizing tools from classical digital signal processing to the cases where the signal domain can be modeled by an arbitrary graph. In this context, the present paper introduces the notion of fractional shift of signals on graphs, which is related to considering a non-integer power of the graph adjacency matrix. Among the results derived throughout this work, we prove that the referred fractional operator can be implemented as a linear and shift-invariant graph filter for any graph and verify its convergence to the classical fractional delay when a directed ring graph is considered. By means of a real-world example, we show that, using the proposed operator, graph filters that approximate an ideal filter better than those designed using the ordinary adjacency matrix can be obtained. An additional example dealing with noise removal from graph signals illustrates the gain provided by the mentioned filter design strategy.

INDEX TERMS Graph signal processing, fractional graph shift operator, graph filter design, noise removal.

I. INTRODUCTION

Over the last decade, theory and applications related to graph signal processing (GSP) have been widely developed and attracted the attention of several scholars [1]–[3]. In short, GSP aims to extend concepts and operations of classical digital signal processing (DSP) to scenarios in which the signals lie over irregular domains. Such scenarios include, for instance, sensors arbitrarily positioned in a geographic region and measuring some climatological variable, points of a three-dimensional cloud representing some virtual object and its attributes, people linked according to their interests and proximity relationships in a social network and so on [4]–[16]. To be more specific, among the issues related to the referred scenarios, one can cite segmentation and attribute compression of 3D point clouds [5], [12], stochastic filtering under asymmetric links in wireless sensor networks [8], community detection in social networks [14], anomalous IoT sensor data detection [15] and traffic prediction via attention networks [16]. It is intuitive that the mentioned examples can be modeled as graphs whose vertices are connected by edges

The associate editor coordinating the review of this manuscript and approving it for publication was Prakasam Periasamy¹.

inferred from a variety of influence or dependency criteria. This contrasts with the discrete-time domain, over which the samples of a signal are equidistantly placed and have left- and right-side immediate neighbors only; something similar happens in the case of digital images, where the pixels are arranged in a regular rectangular grid.

Two main GSP approaches have been consolidated throughout the last years. The first is based on the spectral graph theory and analyzes signals on undirected graphs with real and non-negative edge weights, by using the graph Laplacian to construct a basis for the signal space [17]. The second comes from the algebraic signal processing and uses the weighted adjacency matrix \mathbf{A} as elementary building block [18], [19]; such an approach, which is adopted in this paper, allows to deal with signals defined over both directed and undirected graphs, and with real- and complex-valued edge weights [20]. In any case, the aforementioned approaches have used \mathbf{L} and \mathbf{A} as elementary building blocks because, among other reasons, these matrices are well established in graph theory and allow some meaningful physical interpretation or some parallel with the classical DSP; while \mathbf{A} can be viewed as a generalization of the discrete-time unit shift, \mathbf{L} is a kind of discrete counterpart to the continuous

Laplace-Beltrami (second order) derivative operator on a manifold [21], [22].

Among the research fronts active in GSP, the one that investigates alternatives to the operators usually employed as building blocks to describe graph signals and systems deserves to be highlighted [23]–[29]. In fact, when the purpose is to consider linear operators in this context, any matrix can be chosen to play the role of elementary building block; multiplying a matrix by a graph signal represented as a vector produces another signal whose samples result from a linear combination of the samples of the original signal. In this scope, the use of matrices other than the *standard* adjacency matrix and the Laplacian for the mentioned purpose may be more suitable in specific scenarios and to carry out specific (graph) signal processing tasks. Even when the focus is on designing other graph operators (e.g., the graph Fourier transform), the decision about which elementary operator to use has an impact on the expected results.

Regarding the issue discussed in the last paragraph, some works archived in the GSP literature can be brought to the fore. In [23], for example, the authors propose an isometric graph translation operator that is described in the spectral domain as a phase shifting operator; this operator shares key properties with the time shift and behaves reasonably in the vertex domain. In [24], the authors define an energy-preserving shift operator that satisfy many properties similar to their counterparts in classical signal processing; the GSP framework based on the referred operator enables the signal analysis along a correlation structure defined by a graph shift manifold. In [25] and [26], the authors employ different features associated with a graph to generate a series of shift operators and design a graph-filter-based classifier. Although the proposed method produces better results than those achieved using conventional graph-filter-based classifiers, it requires dealing with a non-convex optimization problem whose solution involves a relatively high computational cost. In [27], motivated by the typical scenario of asymmetric communications in wireless sensor networks, the authors study the optimal design of graph shift operators to perform decentralized subspace projection for asymmetric topologies. Obtaining the referred operators can be performed either by solving an optimization problem or by employing a decentralized algorithm based on an Alternating Direction Method of Multipliers (ADMM). In [28] and [29], the goal is to construct a graph Fourier transform for directed graphs (digraphs), such that the corresponding orthonormal frequency components are as spread as possible in the graph spectral domain. The method uses the Laplacian of an undirected version of the digraph and involves non-convex, orthonormality-constrained optimization problems.

This paper is somehow related to the above mentioned works, since its central theme refers to elementary operators on graphs. To be more specific, we consider the possibility of computing a non-integer power \mathbf{A}^a , $a \in \mathbb{R}$, of the adjacency matrix \mathbf{A} , which is taken as the (unit) graph shift operator [20]. With this, we introduce the notion of fractional

shift (or delay) of signals on graphs, which, to the best of our knowledge, has not yet been addressed in the literature. Differently from the referred papers, in which new operators are created or standard operators are adjusted using strategies potentially expensive from the computational point of view, we propose a relatively simple generalization that fills a theoretical gap concerning the extension to the GSP framework of a well-established concept in the classical signal processing.

In what follows, the main contributions of this paper are listed:

- We introduce the fractional graph shift operator \mathbf{A}^a and discuss its several aspects. More specifically, we demonstrate that \mathbf{A}^a can be computed by using the theory of matrix functions, considering the Jordan decomposition of \mathbf{A} .
- We demonstrate that \mathbf{A}^a acts as a graph filter, give its frequency response and discuss issues related to fractionally shifting graph signals containing discontinuities (Gibbs phenomenon).
- An analogy between the proposed graph fractional operator and that considered in the classical discrete-time case is established; our result suggests that, when a directed ring graph with N vertices is considered, the response of the corresponding graph filter related to \mathbf{A}^a converges to that of the classical fractional delay filter as N grows.
- We determine the polynomial representation of \mathbf{A}^a and, with that, we demonstrate that, for any graph, such a operator can be implemented as a linear and shift-invariant (LSI) graph filter.

This paper is organized as follows. Section II contains a concise review of graph signal processing foundations. In Section III, we introduce the concept of fractional shift on graphs and develop our contributions in detail: we address the computation of \mathbf{A}^a in Subsection III-A, discuss its interpretation in Subsection III-B, demonstrate its consistency with the ideal fractional delay filter in Subsection III-C and determine its polynomial representation in Subsection III-D. Section IV is devoted to numerical results related to the developed theory: we first present a small example regarding the polynomial representation of \mathbf{A}^a in Subsection IV-A; we then consider a real-world graph signal (temperature measured by weather stations) and demonstrate that, using \mathbf{A}^a , we can obtain filters that approximate an ideal filter (in the least-squares sense) better than those designed using \mathbf{A} (Subsections IV-B and IV-C); finally, this possibility is illustrated by means of an example involving the noise removal from the same graph signal (Subsection IV-D). The paper closes with concluding remarks in Section V.

II. FOUNDATIONS OF GRAPH SIGNAL PROCESSING

In this section, the main concepts and definitions related to GSP are briefly presented. As previously remarked, the GSP framework considered in this paper is the one based on the adjacency matrix. In this sense, if one wishes for a

deeper introduction on the matter, please refer to the works of Sandryhaila and Moura [20], [30]–[34].

A. GRAPH SIGNALS AND FILTERS

Let $\mathcal{G} = \{\mathbf{A}, \mathcal{V}\}$ be a graph defined as a set of vertices $\mathcal{V} = \{v_0, v_1, \dots, v_{N-1}\}$ possibly connected by weighted edges. The adjacency matrix \mathbf{A} has in its entry A_{ij} the weight of the edge going from v_j to v_i , with $A_{ij} = 0$ if and only if there is no edge from v_j to v_i .

A signal $\mathbf{x} \in \mathcal{S}$ over the graph \mathcal{G} is defined as

$$\mathbf{x} : \mathcal{V} \rightarrow \mathbb{C}^N, \quad v_n \rightarrow \mathbf{x}(v_n) = x_n, \quad (1)$$

where \mathcal{S} is the space of all signals over \mathcal{G} , that is, the space of discrete functions mapping the set of the N vertices of \mathcal{G} into an N -tuple of complex (or real) values. Given a suitable labelling for the vertices of a graph, a signal \mathbf{x} is represented by the ordered sequence x_n of its values. Graph signals can then be written as ordered N -tuples lying in \mathbb{C}^N or \mathbb{R}^N .

Graphs can be *directed* or *undirected*, depending on whether their edges have or do not have preferred direction. By definition, an adjacency matrix is symmetrical if and only if the corresponding graph is undirected.

A particularly important graph is that shown in Fig. 1, the directed ring graph with edges having unitary weights. Such a graph can be used to model the discrete-time domain with length N and periodic boundary conditions. Its adjacency matrix is given by

$$\mathbf{C} = \begin{bmatrix} & & & & 1 \\ 1 & & & & \\ & \ddots & & & \\ & & \ddots & & \\ & & & 1 & \end{bmatrix}, \quad (2)$$

and plays an essential role in GSP: if a signal $\mathbf{x} = (x_0 \ x_1 \ \dots \ x_{N-1})^T$ defined on a ring graph is left multiplied by the adjacency matrix, one has $\tilde{\mathbf{x}} = (x_{N-1} \ x_0 \ \dots \ x_{N-2})^T$; that is,

$$\tilde{\mathbf{x}} = \mathbf{C}\mathbf{x} \quad (3)$$

is the result of circularly shifting \mathbf{x} to the right. This property suggests to generalize the unit shift of a signal on an arbitrary graph as being the left product by the corresponding adjacency matrix,

$$\tilde{\mathbf{x}} = \mathbf{A}\mathbf{x}, \quad (4)$$

so that \mathbf{A} can be interpreted as the graph shift operator. In fact, this operator is a delay *filter* for graph signals.

A filter for signals on a graph with $|\mathcal{V}| = N$ vertices can be defined as being any matrix $\mathbf{H} \in \mathbb{C}^{N \times N}$ [31]. Therefore, every graph filter is linear. On the other hand,

$$\mathbf{H}\mathbf{A}\mathbf{x} = \mathbf{A}\mathbf{H}\mathbf{x}, \quad \forall \mathbf{x} \in \mathcal{S} \Leftrightarrow \mathbf{H}\mathbf{A} = \mathbf{A}\mathbf{H}, \quad (5)$$

that is, \mathbf{H} is a linear and shift-invariant (LSI) filter if and only if it commutes with the adjacency matrix \mathbf{A} . The following

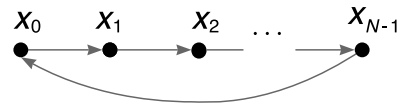


FIGURE 1. A directed ring graph.

theorem establishes an important property satisfied by every LSI filter [31].

Theorem 1: Let \mathbf{A} be the adjacency matrix of a graph. Let us assume that the characteristic polynomial $char_{\mathbf{A}}(x)$ of \mathbf{A} coincides with the respective minimal polynomial $m_{\mathbf{A}}(x)$. Therefore, \mathbf{H} is a LSI filter if and only if \mathbf{H} is a polynomial in \mathbf{A} , i. e.

$$\mathbf{H} = h(\mathbf{A}) = \sum_{\ell=0}^L h_{\ell} \mathbf{A}^{\ell}, \quad (6)$$

where \mathbf{A}^0 is the identity matrix and $L < \deg(m_{\mathbf{A}})$.

The assumption on $char_{\mathbf{A}}(x)$ and $m_{\mathbf{A}}(x)$ in Theorem 1 does not hold for all adjacency matrices \mathbf{A} . Nevertheless, the result in the referred theorem can be extended to all matrices using the concept of *equivalent graph filters*, as clearly explained in [32]. In short, for any graph $\mathcal{G} = \{\mathbf{A}, \mathcal{V}\}$, every LSI filter has polynomial representation in \mathbf{A} . In this sense, Theorem 1 suggests a convenient analogy with the classical DSP, since every filter for discrete-time signals can be represented as polynomials evaluated in z^{-1} , the unit delay, via the z -transform of its impulse response.

B. GRAPH FOURIER TRANSFORM

The graph Fourier transform of a signal is its projection on a basis formed by functions invariant to linear and time-invariant (LTI) filtering [35]. Analogously, the graph Fourier transform (GFT) can be defined as the decomposition of a signal on a basis formed by eigenvectors of LSI filtering. Since LSI filters are polynomials in \mathbf{A} (Theorem 1), and considering that a matrix and its integer powers share the same eigenvectors, the referred basis coincides with that obtained from the decomposition of \mathbf{A} [33]. In this context, if the corresponding graph has N vertices, \mathbf{A} admits the Jordan decomposition

$$\mathbf{A} = \mathbf{V}\mathbf{J}\mathbf{V}^{-1}, \quad (7)$$

in which \mathbf{V} contains the N Jordan (generalized) eigenvectors of \mathbf{A} in its columns,

$$\mathbf{V} = (\mathbf{v}_0 \ \mathbf{v}_1 \ \dots \ \mathbf{v}_{N-1}), \quad (8)$$

and \mathbf{J} is a block diagonal matrix formed of the so-called Jordan blocks. In particular, if \mathbf{A} is diagonalizable, (7) coincides with its eigendecomposition, so that \mathbf{J} reduces to a diagonal matrix whose entries are the eigenvalues of \mathbf{A} .

In this manner, a signal $\mathbf{x} \in \mathcal{S}$ can be decomposed into its components on the basis \mathbf{V} as

$$\begin{aligned} \mathbf{x} &= \hat{x}_0 \mathbf{v}_0 + \dots + \hat{x}_{N-1} \mathbf{v}_{N-1} \\ &= \mathbf{V}(\hat{x}_0 \ \hat{x}_1 \ \dots \ \hat{x}_{N-1})^T \\ &= \mathbf{V}\hat{\mathbf{x}}. \end{aligned} \quad (9)$$

The last expression is then defined as being the synthesis equation of the graph Fourier transform. Consequently, the GFT analysis equation is

$$\widehat{\mathbf{x}} = \mathbf{V}^{-1} \mathbf{x}. \quad (10)$$

For discrete-time signals, it has been remarked that the corresponding domain can be modeled as a directed ring graph with edges having unitary weights and, therefore, with adjacency matrix \mathbf{C} given in (2). Since \mathbf{C} is circulant, it is diagonalized by the discrete Fourier transform (DFT) matrix \mathbf{F} . Thus, one has

$$\mathbf{C} = \mathbf{F}^{-1} \Lambda_{\mathbf{C}} \mathbf{F}, \quad (11)$$

where

$$\Lambda_{\mathbf{C}} = \text{diag} \left(1 \ e^{-j\frac{2\pi}{N}} \ e^{-j\frac{4\pi}{N}} \ e^{-j\frac{6\pi}{N}} \ \dots \ e^{-j\frac{2\pi(N-1)}{N}} \right).$$

In this case, the GFT matrix becomes $\mathbf{V}^{-1} = \mathbf{F}$, evidencing the desirable property that the GFT of discrete-time signals coincides with the DFT.

1) FREQUENCY RESPONSE OF GRAPH FILTERS

In order to understand how a graph filter acts on the GFT domain, identified as frequency domain, (7) and Theorem 1 are used. The response of the filter $\mathbf{H} = \sum_{\ell=0}^L h_{\ell} \mathbf{A}^{\ell}$ to the signal \mathbf{x} is given by

$$\begin{aligned} \mathbf{H} \mathbf{x} &= \sum_{\ell=0}^L h_{\ell} \mathbf{A}^{\ell} \mathbf{x} = \sum_{\ell=0}^L h_{\ell} \left(\mathbf{V} \mathbf{J} \mathbf{V}^{-1} \right)^{\ell} \mathbf{x} \\ &= \mathbf{V} \left(\sum_{\ell=0}^L h_{\ell} \mathbf{J}^{\ell} \right) \mathbf{V}^{-1} \mathbf{x}. \end{aligned} \quad (12)$$

Taking the GFT of both sides of the last equation, one has

$$\mathbf{V}^{-1} \mathbf{H} \mathbf{x} = h(\mathbf{J}) \widehat{\mathbf{x}}, \quad (13)$$

so that the frequency domain equation corresponding to filtering using \mathbf{H} is the multiplication by the matrix $h(\mathbf{J})$, which represents the frequency response of the filter \mathbf{H} .

III. FRACTIONAL SHIFT ON GRAPHS

Since the unit shift of a graph signal can be defined as the product by the adjacency matrix of the graph on which it lies, in this work, we propose to define a fractional shift as the product by a non-integer power of \mathbf{A} . Precisely, the signal \mathbf{x} over the graph $\mathcal{G} = \{\mathbf{A}, \mathcal{V}\}$, after being shifted by $a \in [0, 1]$, is given by

$$\widetilde{\mathbf{x}}_a = \mathbf{A}^a \mathbf{x}. \quad (14)$$

In what follows, we discuss aspects related to the computation of \mathbf{A}^a , the interpretation of its application to a graph signal and the consistency of the proposed operator with the classical DSP approach (ideal fractional delay filter).

A. COMPUTATION OF \mathbf{A}^a

The computation of \mathbf{A}^a can be well established by employing results from the theory of matrix functions [36]. In this context, we are interested in evaluating the originally scalar function $f(t) = t^a$, $a \in \mathbb{R}$, but replacing t with \mathbf{A} . The most direct way to formally define a function like this uses the Jordan canonical form. With this purpose, (7) is reconsidered; in this equation, the block diagonal matrix \mathbf{J} can be written as

$$\mathbf{J} = \text{diag}(\mathbf{J}_1, \mathbf{J}_2, \dots, \mathbf{J}_p), \quad (15)$$

where the k -th Jordan block \mathbf{J}_k is

$$\mathbf{J}_k = \mathbf{J}_k(\lambda_k) = \begin{bmatrix} \lambda_k & 1 & & \\ & \lambda_k & \ddots & \\ & & \ddots & 1 \\ & & & \lambda_k \end{bmatrix} \in \mathbb{C}^{m_k \times m_k} \quad (16)$$

and $m_1 + m_2 + \dots + m_p = N$. Denote by $\lambda_1, \dots, \lambda_s$ the distinct eigenvalues of \mathbf{A} and by n_i the index of λ_i (the order of the largest Jordan block in which λ_i appears). The function f is said to be defined on the spectrum of \mathbf{A} if the values

$$f^{(j)}(\lambda_i), \quad j = 0, 1, \dots, n_i - 1, \quad i = 1, 2, \dots, s, \quad (17)$$

where $f^{(j)}$ denotes the j^{th} derivative of f , exist. This is the case of $f(t) = t^a$. The computation of $f(\mathbf{A}) = \mathbf{A}^a$ can then be carried out as follows.

Definition 1: Let f be defined on the spectrum of $\mathbf{A} \in \mathbb{C}^{N \times N}$ and let \mathbf{A} have the Jordan decomposition (7). Then

$$f(\mathbf{A}) := \mathbf{V} f(\mathbf{J}) \mathbf{V}^{-1} = \mathbf{V} \text{diag}(f(\mathbf{J}_k)) \mathbf{V}^{-1}, \quad (18)$$

where

$$f(\mathbf{J}_k) := \begin{bmatrix} f(\lambda_k) & f'(\lambda_k) & \dots & \frac{f^{(m_k-1)}(\lambda_k)}{(m_k-1)!} \\ & f(\lambda_k) & \ddots & \vdots \\ & & \ddots & f'(\lambda_k) \\ & & & f(\lambda_k) \end{bmatrix}. \quad (19)$$

In the present context, the last definition constitutes a practical way to calculate \mathbf{A}^a , because the Jordan form of the adjacency matrix, being necessary for the definition of the corresponding GFT, may already have been computed and thus be available to be used in (18) and (19).

B. INTERPRETING THE GRAPH FRACTIONAL SHIFT

In order to perform a meaningful interpretation of the graph fractional shift, we consider (14) and the case in which \mathbf{A} is diagonalizable. Using the Jordan decomposition (7), the GFT analysis equation (10) and the computation strategy described in the last subsection, we can write

$$\begin{aligned} \mathbf{A}^a \mathbf{x} &= \mathbf{V} \Lambda^a \mathbf{V}^{-1} \mathbf{x} = \mathbf{V} \begin{bmatrix} \lambda_1^a & & \\ & \ddots & \\ & & \lambda_N^a \end{bmatrix} \widehat{\mathbf{x}} \\ &= \mathbf{V} (\widehat{\mathbf{h}}_a \odot \widehat{\mathbf{x}}) = \text{GFT}^{-1} \{ \widehat{\mathbf{h}}_a \odot \widehat{\mathbf{x}} \}, \end{aligned} \quad (20)$$

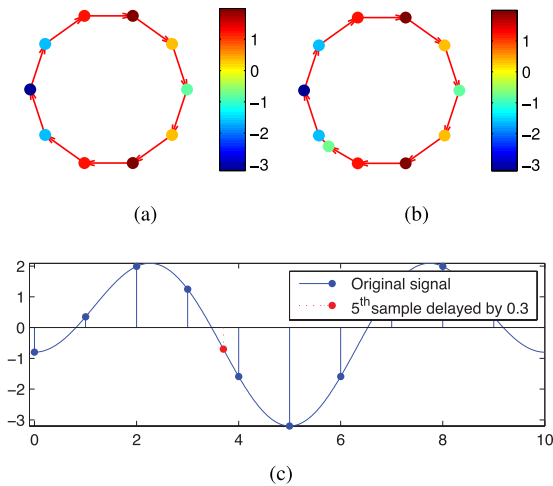


FIGURE 2. Fractional shift by $\alpha = 0.3$ of a sample of a signal on a directed ring graph with unit weights. (a) Original signal on a directed ring graph. (b) Graph in which the 5th sample delayed by $\alpha = 0.3$ appears as an interpolated sample between the 4th and the 5th samples of the original signal. (c) Original discrete signal and the delayed sample.

where $\hat{\mathbf{h}}_a := (\lambda_1^a \dots \lambda_N^a)$ and \odot represents the point-wise vector product.

Equation (20) shows that \mathbf{A}^a is a graph filter with frequency response $\text{diag}(\hat{\mathbf{h}}_a)$; moreover, if \mathbf{x} is an N -point discrete-time signal (case in which the GFT coincides with the DFT), one observes that the filter in the DFT domain is the vector $\hat{\mathbf{h}}_a$ itself. In this case, it has been discussed that the adjacency matrix of the respective graph is diagonalized according with (11), where $\Lambda_{\mathbf{C}}$ has as entries the N roots of unity. The fact that the matrix of eigenvectors of \mathbf{C} is the Fourier matrix imposes a specific order of the eigenvalues in $\Lambda_{\mathbf{C}}$, so that the vector $\hat{\mathbf{h}}_a$ is

$$\hat{\mathbf{h}}_a = (1 \ W_N^a \ W_N^{2a} \ \dots \ W_N^{aR} \ W_N^{-aR'} \ W_N^{a(-R'+1)} \ \dots \ W_N^{-a}),$$

where $W_N = e^{-j\frac{2\pi}{N}}$ and

$$\begin{cases} R = \frac{N-1}{2} \text{ and } R' = R, & \text{if } N \text{ is odd,} \\ R = \frac{N}{2} - 1 \text{ and } R' = R + 1, & \text{if } N \text{ is even,} \end{cases} \quad (21)$$

$n = 0, 1, \dots, N - 1$. It can be shown that the inverse DFT of $\hat{\mathbf{h}}_a$ has components given by (22), as shown at the bottom of the next page.

The product by a fractional power of the adjacency matrix produces the effect illustrated in Fig. 2, for a directed ring graph; it can be seen, for example, how the 5th sample of the signal shifted by $a = 0.3$ coincides with the value of the continuous-time signal at the same position. On the other hand, the analysis we can perform by observing the *irregular* graph in Fig. 3 is mostly visual; as we vary the fractional parameter from 0 (original signal) to 1, we see in the intermediate snapshots how the signal gradually spreads out from the vertices where, originally, there were already non-zero samples. In this scope, although we employ terms such as delay and shift, which are inherited from classical signal processing, the process observed in the figure looks more like a

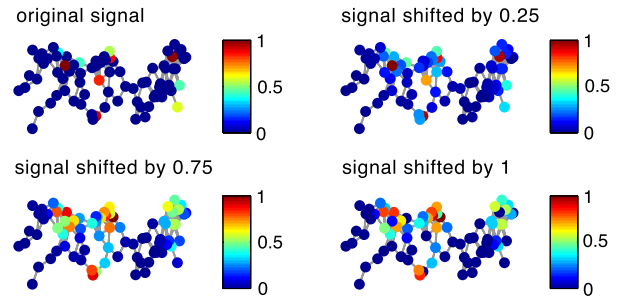


FIGURE 3. Fractional shift of a signal, (originally) with 10 non-zero samples, defined on a graph formed by 80 cities of Pernambuco state, Brazil. Note that the shifted signal is similar to the original signal, if α is close to 0, and similar to the unit-shifted signal, if α is close to 1.

kind of (fractional) diffusion. In fact, diffusion on graphs have been widely studied [37]–[39]; it is usually described in terms of a system of ordinary differential equations in time, with the Laplacian matrix of the graph as the coefficient matrix. Fractional diffusion has been used to model certain phenomena that allow long-range interactions and are non-local in nature [40]–[43]. In future works, we intend to investigate the possible relationships between the operator proposed in this paper and the mathematical tools for fractional diffusion in networks.

Finally, we draw attention to the fact that the signal to be shifted has to be band-limited (see Fig. 4a). If the signal has abrupt changes in its sample values, this can be viewed as a kind of discontinuity and represents high frequency components, when compared to the predominantly smooth behavior of the signal (see Fig. 4b). As a consequence, we can observe considerable fluctuations around the disparate samples when the signal is fractionally delayed, an effect similar to the Gibbs phenomenon.

C. CONSISTENCY WITH CLASSICAL APPROACH: THE IDEAL FRACTIONAL DELAY FILTER

In the classical approach to the problem of fractionally shifting a discrete-time signal, the continuous-time version of the signal can be reconstructed by shifting and then resampling with the same sample period [44], [45]. Due to the Nyquist-Shannon Theorem, this procedure requires that the signal is band-limited. In this context, it can be shown that, if a discrete-time signal \mathbf{x} is band-limited, its version shifted by $a \in [0, 1]$ is

$$x[n - a] = \sum_k x[k] \text{sinc}(n - k - a),$$

so that the (ideal low-pass) filter used to perform the referred shift has components

$$h_{LPF}[n] = \text{sinc}(n - a). \quad (23)$$

The filter \mathbf{h}_{LPF} is non-causal and unstable (it is not BIBO – bounded input, bounded output, because its impulse response has infinite energy) and, therefore, it is not physically realizable. In this way, fractional delay filter implementations should just *approximate* \mathbf{h}_{LPF} as much as possible.

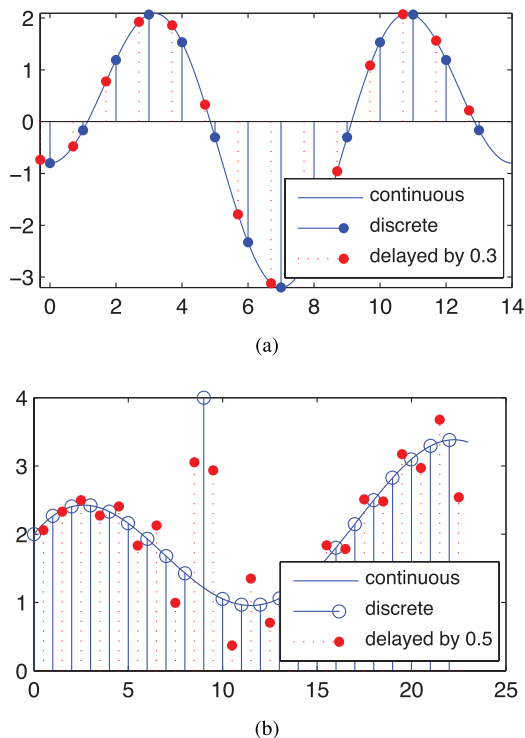


FIGURE 4. Fractional shift for a signal (a) without and (b) with abrupt variations (discontinuities).

In order to evaluate how close to $h_{LPF}[n] = \text{sinc}(n-a)$, $0 \leq a \leq 1$, is $h_a[n]$, for odd N (see the first row of (22)), the point-wise difference between these signals has been computed for different values of $N \in [10^1, 10^6]$. In Fig. 5, we show the relative error (ratio between the energy of the error ($\mathbf{h}_a - \mathbf{h}_{LPF}$) and that of \mathbf{h}_{LPF}), in terms of N and a .

The result suggests that, in fact, \mathbf{h}_a converges in the mean in ℓ^2 to \mathbf{h}_{LPF} as N grows, with relative error less than 5% for $N \approx 30$. Moreover, the error is greater when a is close to 0.5, being negligible or null when a is an integer. In fact, the error is exactly zero for $a = 0$ (or $a = 1$) and $n = a$, since

$$\lim_{n \rightarrow a} h_a[n] = 1 \Rightarrow \lim_{n \rightarrow a} (h_a[n] - \text{sinc}(n-a)) = 0. \quad (24)$$

The same result is obtained for even N , starting from the second row of (22). When a is non-integer, $h_a[n]$ is complex, with imaginary part of constant modulus for a fixed a . Considering the corresponding real part only, the error was smaller than that taking into account also the contribution of the imaginary part. Fig. 6 and Fig. 7 show that the errors with and without the imaginary part equally decay as N grows, but, using the real part only, the results are significantly better.

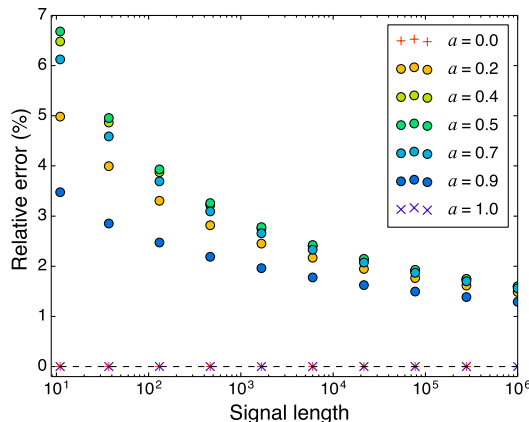


FIGURE 5. Percent error (normalized by the energy of \mathbf{h}_{LPF}) of \mathbf{h}_a related to \mathbf{h}_{LPF} , for different (odd) values of N and the fractional shift parameter a .

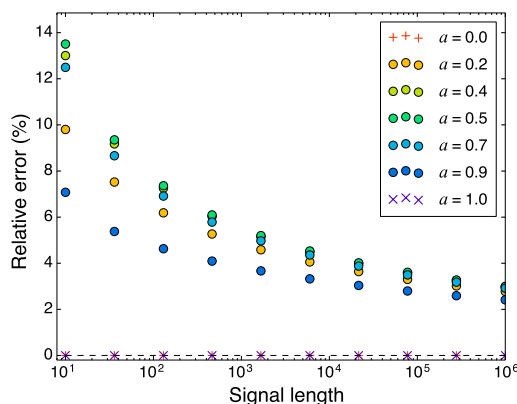


FIGURE 6. Relative mean error between $\text{Re}(\mathbf{h}_a)$ and \mathbf{h}_{LPF} for N even, in terms of the fractional shift parameter a .

D. POLYNOMIAL REPRESENTATION

The fractional shift matrix \mathbf{A}^a necessarily commutes with \mathbf{A} , because $\mathbf{A}^a \mathbf{A} = \mathbf{A}^{1+a} = \mathbf{A} \mathbf{A}^a$, so that \mathbf{A}^a is an LSI filter for signals on graphs having \mathbf{A} as adjacency matrix (see (5)). Therefore, according to Theorem 1, \mathbf{A}^a admits a polynomial representation like the one given in (6). In what follows, we evaluate such a possibility for directed ring graphs and for arbitrary graphs.

1) DIRECTED RING GRAPHS

The adjacency matrix \mathbf{C} in (2) of the directed ring graph with unitary weights satisfies $\text{char}_{\mathbf{C}} = m_{\mathbf{C}}$ (due to the fact that the eigenvalues of \mathbf{C} are distinct). Therefore $\mathbf{H} = \mathbf{C}^a$ can be directly expressed as a polynomial of degree up to $(N - 1)$ in \mathbf{C} . In order to do this, we consider (11) and the fact that $\mathbf{F}^{-1} = \mathbf{F}^H$, with H indicating the conjugate transpose. This

$$h_a[n] = \begin{cases} \frac{1}{N} \frac{\sin(\pi(n-a))}{\sin\left(\frac{\pi}{N}(n-a)\right)}, & \text{if } N \text{ is odd,} \\ \frac{1}{N} \cot\left(\frac{\pi}{N}(n-a)\right) \sin(\pi(n-a)) + \frac{j}{N} (-1)^n \sin(\pi a), & \text{if } N \text{ is even.} \end{cases} \quad (22)$$

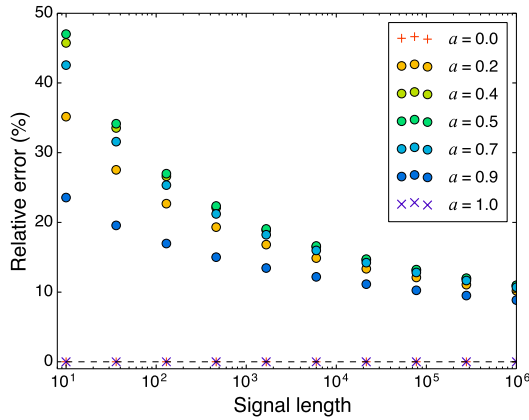


FIGURE 7. Modulus of the relative mean error between \mathbf{h}_a and \mathbf{h}_{LPF} for N even, in terms of the fractional shift parameter α .

allows to show that $\mathbf{C}^\alpha = \mathbf{F}^H \Lambda_{\mathbf{C}}^\alpha \mathbf{F}$ is a circulant matrix with the first column given by \mathbf{h}_a in (22). Moreover, since the left product of a matrix by \mathbf{C} produces a circular down-shift in each column of the matrix, the N powers of \mathbf{C} form a basis for the space of $N \times N$ circulant matrices (note that $\mathbf{C}^N = \mathbf{C}^0$ is the identity matrix). From the above, we conclude that the coefficients of the polynomial representation of \mathbf{C}^α are the entries of \mathbf{h}_a , i. e.

$$\mathbf{H} = \mathbf{C}^\alpha = \sum_{\ell=0}^{N-1} h_a[\ell] \mathbf{C}^\ell. \quad (25)$$

2) ARBITRARY GRAPHS

In order to demonstrate how to obtain the polynomial representation of $\mathbf{H} = \mathbf{A}^\alpha$ for arbitrary graphs, we consider another strategy to compute matrix functions. We first remember that, by definition, the minimal polynomial $m_{\mathbf{A}}(t)$ of \mathbf{A} is the unique monic polynomial of lowest degree such that $m_{\mathbf{A}}(\mathbf{A}) = \mathbf{0}$. By considering the Jordan canonical form of \mathbf{A} , it can be seen that

$$m_{\mathbf{A}}(t) = \prod_{i=1}^s (t - \lambda_i)^{n_i}. \quad (26)$$

It follows immediately that $m_{\mathbf{A}}$ is zero on the spectrum of \mathbf{A} , that is, the values computed in (17) are all zero for $f(t) = m_{\mathbf{A}}(t)$. Given any polynomial p and any matrix $\mathbf{A} \in \mathbb{C}^{N \times N}$, p is clearly defined on the spectrum of \mathbf{A} and $p(\mathbf{A})$ can be defined by substitution. For polynomials p and q , $p(\mathbf{A}) = q(\mathbf{A})$ if and only if p and q take the same values on the spectrum. Thus the matrix $p(\mathbf{A})$ is completely determined by the values of p on the spectrum of \mathbf{A} . The following definition can then be established.

Definition 2: Let f be defined on the spectrum of $\mathbf{A} \in \mathbb{C}^{N \times N}$. Then $f(\mathbf{A}) := p(\mathbf{A})$, where p is the unique polynomial of degree less than $\sum_{i=1}^s n_i$ (which is the degree of the minimal polynomial) that satisfies the interpolation conditions

$$p^{(j)}(\lambda_i) = f^{(j)}(\lambda_i), \quad j = 0 : n_i - 1, \quad i = 1 : s. \quad (27)$$

The polynomial p above is known as the Hermite interpolating polynomial. In particular, if $n_i = 1, i = 1, \dots, s, p$ corresponds to the Lagrange interpolating polynomial

$$p(t) = \sum_{i=1}^s f(\lambda_i) l_i(t), \quad l_i(t) = \prod_{j=1, j \neq i}^s \left(\frac{t - \lambda_j}{\lambda_i - \lambda_j} \right). \quad (28)$$

In any case, the results briefly presented above lead us to conclude that \mathbf{A}^α can be expressed as a polynomial in \mathbf{A} and, therefore, according to Theorem 1, the fractional shift of a graph signal can be implemented as a LSI graph filter.

IV. NUMERICAL RESULTS

In the last section, we have discussed the effect of applying a fractional shift to a graph signal and demonstrated that \mathbf{A}^α admits a polynomial representation. In the first part of this section, we develop a small numerical example to illustrate how the referred representation can be obtained. Secondly, we consider a possibility that, for practical purposes, seems to allow better exploiting the potential for generalization of the proposed fractional operator: replacing \mathbf{A} with \mathbf{A}^α in (6) when designing a graph filter. Naturally, the resulting filter, being a polynomial in \mathbf{A}^α , could also be expressed as a polynomial in \mathbf{A} and, therefore, it is a LSI filter.

A. EXAMPLE: POLYNOMIAL REPRESENTATION OF \mathbf{A}^α

The graph considered in this example is shown in Fig. 8 and has adjacency matrix

$$\mathbf{A} = \begin{bmatrix} 5 & 4 & 2 & 1 \\ 0 & 1 & -1 & -1 \\ -1 & -1 & 3 & 0 \\ 1 & 1 & -1 & 2 \end{bmatrix}. \quad (29)$$

The entries of \mathbf{A} in (29) were chosen so that the Jordan decomposition of such a matrix had integer entries only. The referred decomposition is written using matrices

$$\mathbf{V} = \begin{bmatrix} -1 & 1 & 1 & 1 \\ 1 & -1 & 0 & 0 \\ 0 & 9 & -1 & 0 \\ 0 & 1 & 1 & 0 \end{bmatrix},$$

$$\mathbf{V}^{-1} = \begin{bmatrix} 0 & 1 & 1 & 1 \\ 0 & 0 & 1 & 1 \\ 0 & 0 & -1 & 0 \\ 1 & 1 & 1 & 0 \end{bmatrix}$$

and

$$\mathbf{J} = \begin{bmatrix} 1 & 0 & 0 & 0 \\ 0 & 2 & 0 & 0 \\ 0 & 0 & 4 & 1 \\ 0 & 0 & 0 & 4 \end{bmatrix}. \quad (30)$$

Considering $f(t) = t^{0.3}$ and Definition 1, $f(\mathbf{A}) = \mathbf{A}^{0.3}$ can be computed according to

$$\mathbf{A}^{0.3} = \mathbf{V} \begin{bmatrix} f(1) & 0 & 0 & 0 \\ 0 & f(2) & 0 & 0 \\ 0 & 0 & f(4) & f'(4) \\ 0 & 0 & 0 & f(4) \end{bmatrix} \mathbf{V}^{-1},$$

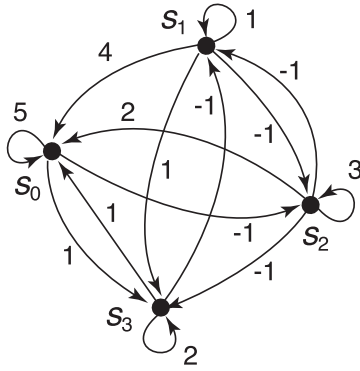


FIGURE 8. Directed graph used to illustrate how the corresponding fractional shift operator can be computed and represented in polynomial form.

which gives

$$\mathbf{A}^{0.3} = \begin{bmatrix} 1.6294 & 0.6294 & 0.3448 & 0.2311 \\ 0 & 1.0000 & -0.2311 & -0.2311 \\ -0.1137 & -0.1137 & 1.4020 & 0 \\ 0.1137 & 0.1137 & -0.1709 & 1.2311 \end{bmatrix}.$$

The same result can be achieved by using Definition 2, which gives

$$\begin{aligned} p(\mathbf{A}) &= f(\mathbf{A}) = \mathbf{A}^{0.3} \\ &= 0.6688\mathbf{I} + 0.3915\mathbf{A} - 0.0654\mathbf{A}^2 + 0.0051\mathbf{A}^3, \end{aligned}$$

the polynomial representation of $\mathbf{A}^{0.3}$.

B. LEAST-SQUARE APPROXIMATION OF LSI FILTERS

Before developing a numerical example illustrating the use of \mathbf{A}^a to filter graph signals, we first review a simple design technique that are least-squares approximations of ideal LSI filters [34]. Such a method consists of defining the (ideal) filter by specifying the values of $h(\lambda_i)$ (filter response in each eigenvalue of the shift operator), instead of determining the values of h_ℓ (filter coefficients). Describing the frequency response of the filter for each eigenvalue λ_i , we obtain the linear system of equations

$$\begin{aligned} h(\lambda_0) &= \alpha_0, \\ h(\lambda_1) &= \alpha_1, \\ &\vdots \\ h(\lambda_{N-1}) &= \alpha_{N-1}, \end{aligned} \quad (31)$$

or, since $h(\cdot)$ is a polynomial of degree L ,

$$\begin{aligned} h_0 + h_1\lambda_0 + \dots + h_L\lambda_0^L &= \alpha_0, \\ h_0 + h_1\lambda_1 + \dots + h_L\lambda_1^L &= \alpha_1, \\ &\vdots \\ h_0 + h_1\lambda_{N-1} + \dots + h_L\lambda_{N-1}^L &= \alpha_{N-1}. \end{aligned} \quad (32)$$

Using a Vandermonde matrix constructed from the eigenvalues λ_i , the system (32) can be written in matrix

form as

$$\begin{bmatrix} 1 & \lambda_0 & \lambda_0^2 & \dots & \lambda_0^L \\ 1 & \lambda_1 & \lambda_1^2 & \dots & \lambda_1^L \\ \vdots & \vdots & \vdots & \ddots & \vdots \\ 1 & \lambda_{N-1} & \lambda_{N-1}^2 & \dots & \lambda_{N-1}^L \end{bmatrix} \begin{bmatrix} h_0 \\ h_1 \\ \vdots \\ h_L \end{bmatrix} = \begin{bmatrix} \alpha_0 \\ \alpha_1 \\ \vdots \\ \alpha_{N-1} \end{bmatrix}. \quad (33)$$

More specifically, if one desires to design a low-pass filter (LPF) whose cutoff frequency is $\lambda_{i_{\text{cut}}}$, one could set

$$\begin{cases} \alpha_i = 1, & \text{for } j = 0, \dots, i_{\text{cut}}, \\ \alpha_i = 0, & \text{for } j = i_{\text{cut}} + 1, \dots, N - 1. \end{cases} \quad (34)$$

Since one generally has $N \geq L + 1$, the system of equations (33) is *overdetermined* and does not have an exact solution. A possible strategy is to find coefficients h_ℓ , $\ell = 0, \dots, L - 1$, that minimize, in the least-squares sense, the deviation from the ideal filter response. This corresponds to solve the optimization problem

$$\min_{\{h_\ell\}_{0, \dots, L-1}} \left(\sum_{n=0}^{N-1} h(\lambda_n) - \alpha_n \right)^2. \quad (35)$$

Our proposal is to replace \mathbf{A} with \mathbf{A}^a in (6). If this is performed, the only adjustment needed in the technique described above consists of replacing the eigenvalues λ_i with their a^{th} powers λ_i^a in (32). The effect of such a substitution is illustrated and evaluated in what follows.

C. EXAMPLE: LS APPROXIMATION USING \mathbf{A}^a

In this example, we consider a network formed by 230 weather stations that measure daily temperature across the United States [46]. Such stations are represented by the vertices of an undirected graph whose edges have been established by using the 8-nearest neighbor criterion. The edge connecting vertices v_n and v_m is weighted according with

$$\mathbf{A}_{n,m} = \frac{e^{-d_{n,m}^2}}{\sqrt{\sum_{k \in \mathcal{N}_n} e^{-d_{n,k}^2} \sum_{\ell \in \mathcal{N}_m} e^{-d_{n,\ell}^2}}}, \quad (36)$$

where $d_{n,m}$ denotes the geodesical distance between the n^{th} and the m^{th} sensors. The snapshot of all measurements taken on February 1st, 2003 forms the signal indexed by the referred graph, which is shown in Fig. 9. From the GFT of the signal, which is plotted in Fig. 10, it can be seen that its spectral content is concentrated in the low graph frequencies. Note that such frequencies correspond to the eigenvalues of \mathbf{A} , which are marked along the horizontal axis of the figure; additionally, the referred marking accompanies the fact that low (resp. high) graph frequencies are associated with higher (resp. lower) eigenvalues [34].

We then use the strategy explained in Subsection IV-B to design a filter that approximates an ideal low-pass filter with $\lambda_{i_{\text{cut}}} = 0.2$. In this case, $i_{\text{cut}} = 39$ so that the 40 lowest graph frequencies are (ideally) preserved after the signal is

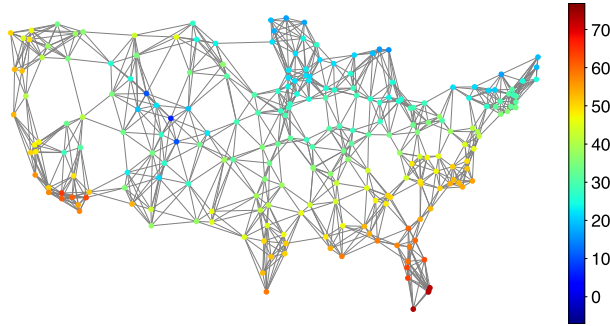


FIGURE 9. Graph of a network formed by 230 weather stations measuring the temperature across the United States. The snapshot of all measurements taken on February 1st, 2003 is the corresponding graph signal.

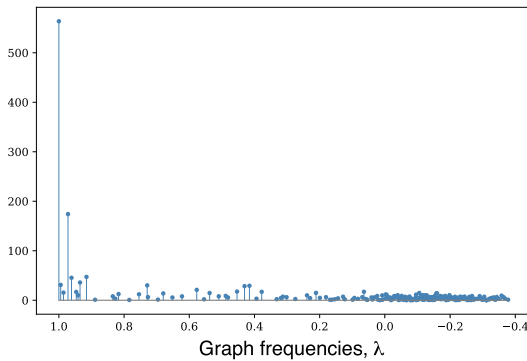


FIGURE 10. Magnitude of the graph Fourier transform of the signal in Fig 9. The graph frequencies correspond to the eigenvalues of \mathbf{A} ; low (resp. high) graph frequencies are associated with higher (resp. lower) eigenvalues.

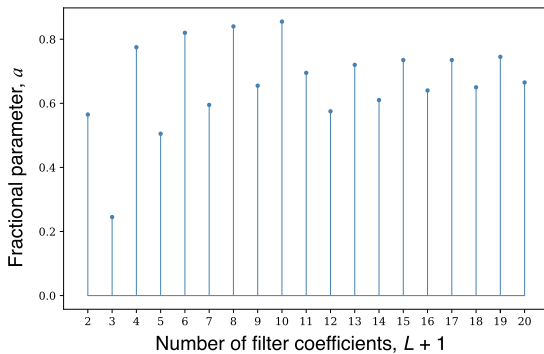


FIGURE 11. Fractional parameters providing the minimum approximation errors, for different values of L , between the ideal LPF and the filter designed by using the fractional graph shift operator \mathbf{A}^a .

filtered. We considered approximations with L ranging from 1 to 19, that is, filters with 2 to 20 coefficients. For each of these values, we varied the fractional parameter a from 0 to 1 and, in (33), after replacing λ_i with λ_i^a , $i = 0, 1, \dots, N - 1$, and solving (35),¹ we registered the value of a providing the minimum error between the designed filter and the ideal filter. At the end of this procedure, the graph shown in Fig. 11

¹The optimization problem (35) has been solved using the Linear Algebra module *linalg* for Scipy, a free and open-source Python library used for scientific and technical computing. In all experiments performed, the least mean squares algorithm converged and the time required for this was negligible, considering the addressed application scenario.

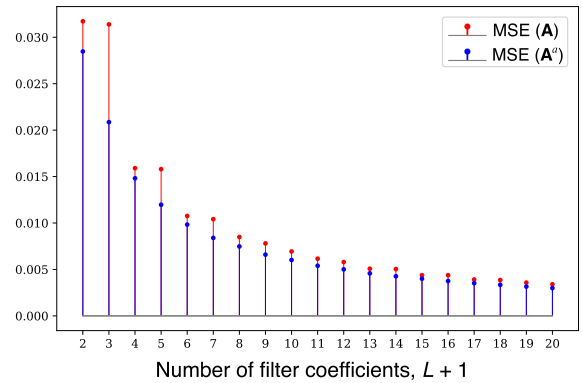


FIGURE 12. Minimum approximation (mean squared) errors, for different values of L , between the ideal LPF and the filters designed by using the fractional graph shift operator \mathbf{A}^a and the non-fractional operator \mathbf{A} .

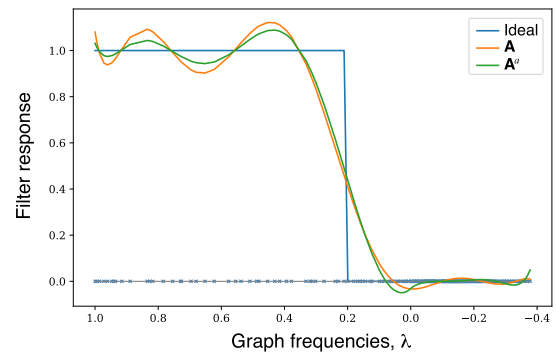


FIGURE 13. Ideal filter response superimposed on the responses obtained when \mathbf{A} and \mathbf{A}^a , $a = 0.855$, are used to design a filter with $L + 1 = 10$ coefficients.

was produced. Observing the figure, we verify that, for any value of L , the best approximation is provided when $a \neq 1$. This is enough to conclude that, for the graph considered in the example, the use of a fractional version \mathbf{A}^a , $a \neq 1$, of \mathbf{A} always provides a better result than the one obtained with the non-fractional matrix. A visual comparison between these alternatives can be performed from Fig. 12, where we show the (minimum) errors we have just referred to together with the errors when the original (non-fractional) matrix \mathbf{A} is employed.

In Fig. 13, we can observe the ideal filter response superimposed on the responses obtained when \mathbf{A} and \mathbf{A}^a are used to design a filter with $L + 1 = 10$ coefficients. In this case, the fractional parameter providing the minimum error is $a = 0.855$. In the figure, we notice that the filter designed with \mathbf{A}^a has fluctuations that deviate less from the ideal filter, when compared to those related to the filter designed using \mathbf{A} . This can be observed mainly in the passband and constitutes a visual result coherent with the obtained approximation errors. Graphs with similar behaviour are obtained for other values L .

D. EXAMPLE: NOISE REMOVAL

In this example, we start from the same graph signal considered in Subsection IV-C. We add to the samples of the referred signal random uniformly-distributed values whose amplitude

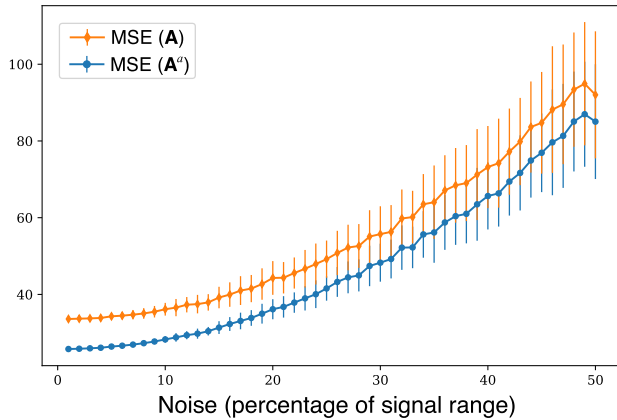


FIGURE 14. Reconstruction (mean squared) errors after a noise removal procedure is performed by using graph filters with $L + 1 = 10$ coefficients and designed from \mathbf{A} and \mathbf{A}^a , $a = 0.855$.

corresponds to a percentage of the range of the signal itself. Such a synthetic noise addition is intended to simulate what happens in many practical scenarios, in which measurements performed on a sensor network are subject to different sources of distortion. The resulting noisy signal is then filtered by using the filters shown in Fig. 13, as an attempt to reduce the influence of the noise and recover the original signal.

In our experiment, we varied the aforementioned percentage from 1% to 50% and, for each of these values, we generated 100 noisy signals. We then filtered such signals and compared the resulting signals with the original (non-noisy) signal by the computation of mean-squared errors. The results, which can be viewed in Fig. 14, show that the filter designed using $\mathbf{A}^{0.855}$ allows to recover the signal with average reconstruction error always smaller than that related to the filter designed using \mathbf{A} . In this context, it is relevant to remark that the (best) fractional parameter $a = 0.855$ has been found using the strategy described in the second paragraph of Subsection IV-C, which depends on the error between the designed filter and the ideal filter only. Therefore, the referred choice does not require us to know the original signal, which is not available in the real-world. This illustrates the potential gain that can be achieved, in this application scenario, when considering the possibility of fractionalization of the graph shift operator.

Finally, it is also interesting to mention that only one or a few nodes could have had their measurements corrupted by noise or changed due to other factors; this would represent a scenario in which certain sensors would be malfunctioning. In order to obtain some preliminary results taking into account the above described assumption, we carried out additional simulations. To be more specific, we basically repeated our previous tests, but assuming that only a number from 1 to 12 nodes had their values nullified or increased by 20 times. We then performed a low-pass filtering, expecting that the high-frequency component associated with the referred measurement changes would be attenuated and that the smooth behavior of the signal would be recovered. In general, the results obtained using the proposed fractional operator were

better or at least equivalent to those obtained with the corresponding ordinary operator. In a future work, we intend to address this issue in more detail.

V. CONCLUDING REMARKS

In this paper, we have investigated the fractional shift of graph signals. The key-point for our developments is the fact that, in the GSP theory, the unit shift is defined from the adjacency matrix of a graph. Interpreting the fractional shift as a filtering operation, we demonstrated that, for ring graphs, its application produces the expected effect of approximating the classical ideal interpolating filter, exhibiting satisfactory results for band-limited signals. We have also shown that the referred fractional operator can be implemented as an LSI graph filter for arbitrary graphs and developed real-world examples that illustrated the benefits of using \mathbf{A}^a to design graph filters for noise removal. Our current investigations include the study of the fractionalization of other operators on graphs (e.g., graph Fourier transform and Laplacian), other types of generalization for the same operators and further applications of the fractional graph shift. In particular, we have been studying the use of \mathbf{A}^a to design filters for anomaly detection on graphs (malfunctioning nodes in a sensor network, for instance) and evaluating the feasibility of introducing a kind of generalized degree index, so that long range interactions can be considered.

REFERENCES

- [1] A. Ortega, P. Frossard, J. Kovačević, J. M. F. Moura, and P. Vandergheynst, "Graph signal processing: Overview, challenges, and applications," *Proc. IEEE*, vol. 106, no. 5, pp. 808–828, May 2018.
- [2] P. M. Djuric and C. Richard, *Cooperative and Graph Signal Processing: Principles and Applications*. Academic, 2018.
- [3] G. Ribeiro and J. Lima, "Graph signal processing in a nutshell," *J. Commun. Inf. Syst.*, vol. 33, no. 1, pp. 219–233, 2018.
- [4] S. Chen, A. Sandryhaila, J. M. F. Moura, and J. Kovacevic, "Signal denoising on graphs via graph filtering," in *Proc. IEEE Global Conf. Signal Inf. Process. (GlobalSIP)*, Dec. 2014, pp. 872–876.
- [5] C. Zhang, D. Florencio, and C. Loop, "Point cloud attribute compression with graph transform," in *Proc. IEEE Int. Conf. Image Process. (ICIP)*, Oct. 2014, pp. 2066–2070.
- [6] K. Benzi, V. Kalofolias, X. Bresson, and P. Vandergheynst, "Song recommendation with non-negative matrix factorization and graph total variation," in *Proc. IEEE Int. Conf. Acoust., Speech Signal Process. (ICASSP)*, Mar. 2016, pp. 2439–2443.
- [7] W. Huang, A. G. Marques, and A. R. Ribeiro, "Rating prediction via graph signal processing," *IEEE Trans. Signal Process.*, vol. 66, no. 19, pp. 5066–5081, Oct. 2018.
- [8] L. Ben Saad and B. Beferull-Lozano, "Stochastic graph filtering under asymmetric links in wireless sensor networks," in *Proc. IEEE 19th Int. Workshop Signal Process. Adv. Wireless Commun. (SPAWC)*, Jun. 2018, pp. 1–5.
- [9] X. Jiang, Z. Tian, and K. Li, "A graph-based approach for missing sensor data imputation," *IEEE Sensors J.*, vol. 21, no. 20, pp. 23133–23144, Oct. 2021.
- [10] F. Gama, E. Isufi, A. Ribeiro, and G. Leus, "Controllability of bandlimited graph processes over random time varying graphs," *IEEE Trans. Signal Process.*, vol. 67, no. 24, pp. 6440–6454, Dec. 2019.
- [11] Y. Liu, L. Yang, K. You, W. Guo, and W. Wang, "Graph learning based on spatiotemporal smoothness for time-varying graph signal," *IEEE Access*, vol. 7, pp. 62372–62386, 2019.
- [12] S. Zhang, S. Cui, and Z. Ding, "Hypergraph spectral clustering for point cloud segmentation," *IEEE Signal Process. Lett.*, vol. 27, pp. 1655–1659, 2020.

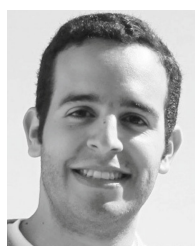
- [13] F. A. B. S. Ferreira and J. B. Lima, "A robust 3D point cloud watermarking method based on the graph Fourier transform," *Multimedia Tools Appl.*, vol. 79, nos. 3–4, pp. 1921–1950, Jan. 2020.
- [14] Q. Zhang, V. Y. F. Tan, and C. Suh, "Community detection and matrix completion with social and item similarity graphs," *IEEE Trans. Signal Process.*, vol. 69, pp. 917–931, 2021.
- [15] Z. Xiao, H. Fang, and X. Wang, "Anomalous IoT sensor data detection: An efficient approach enabled by nonlinear frequency-domain graph analysis," *IEEE Internet Things J.*, vol. 8, no. 5, pp. 3812–3821, Mar. 2021.
- [16] B. Sun, D. Zhao, X. Shi, and Y. He, "Modeling global spatial-temporal graph attention network for traffic prediction," *IEEE Access*, vol. 9, pp. 8581–8594, 2021.
- [17] D. I. Shuman, S. K. Narang, P. Frossard, A. Ortega, and P. Vandergheynst, "The emerging field of signal processing on graphs: Extending high-dimensional data analysis to networks and other irregular domains," *IEEE Signal Process. Mag.*, vol. 30, no. 3, pp. 83–98, Apr. 2013.
- [18] M. Püschel and J. M. F. Moura, "Algebraic signal processing theory: Foundation and 1-D time," *IEEE Trans. Signal Process.*, vol. 56, no. 8, pp. 3572–3585, Aug. 2008.
- [19] M. Püschel and J. M. F. Moura, "Algebraic signal processing theory: 1-D space," *IEEE Trans. Signal Process.*, vol. 56, no. 8, pp. 3586–3599, May 2008.
- [20] A. Sandryhaila and J. M. F. Moura, "Big data analysis with signal processing on graphs: Representation and processing of massive data sets with irregular structure," *IEEE Signal Process. Mag.*, vol. 31, no. 5, pp. 80–90, Sep. 2014.
- [21] F. R. K. Chung, *Spectral Graph Theory*, no. 92. Providence, RI, USA: American Mathematical Society, 1997.
- [22] R. R. Coifman, S. Lafon, A. B. Lee, M. Maggioni, B. Nadler, F. Warner, and S. W. Zucker, "Geometric diffusions as a tool for harmonic analysis and structure definition of data: Diffusion maps," *Proc. Nat. Acad. Sci. USA*, vol. 102, no. 21, pp. 7426–7431, 2005.
- [23] B. Girault, P. Goncalves, and E. Fleury, "Translation on graphs: An isometric shift operator," *IEEE Signal Process. Lett.*, vol. 22, no. 12, pp. 2416–2420, Dec. 2015.
- [24] A. Gavili and X.-P. Zhang, "On the shift operator, graph frequency, and optimal filtering in graph signal processing," *IEEE Trans. Signal Process.*, vol. 65, no. 23, pp. 6303–6318, Dec. 2017.
- [25] J. Fan, C. Tepedelenlioglu, and A. Spanias, "Graph filtering with multiple shift matrices," in *Proc. IEEE Int. Conf. Acoust., Speech Signal Process. (ICASSP)*, May 2019, pp. 3557–3561.
- [26] J. Fan, C. Tepedelenlioglu, and A. Spanias, "Global optimization of graph filters with multiple shift matrices," in *Proc. 53rd Asilomar Conf. Signals, Syst., Comput.*, Nov. 2019, pp. 2082–2086.
- [27] S. Mollaebrahim and B. Beferull-Lozano, "Design of asymmetric shift operators for efficient decentralized subspace projection," *IEEE Trans. Signal Process.*, vol. 69, pp. 2056–2069, 2021.
- [28] R. Shafipour, A. Khodabakhsh, G. Mateos, and E. Nikolova, "Digraph Fourier transform via spectral dispersion minimization," in *Proc. IEEE Int. Conf. Acoust., Speech Signal Process. (ICASSP)*, Apr. 2018, pp. 6284–6288.
- [29] R. Shafipour, A. Khodabakhsh, G. Mateos, and E. Nikolova, "A directed graph Fourier transform with spread frequency components," *IEEE Trans. Signal Process.*, vol. 67, no. 4, pp. 946–960, Feb. 2019.
- [30] S. Chen, R. Varma, A. Sandryhaila, and J. Kovačević, "Discrete signal processing on graphs: Sampling theory," *IEEE Trans. Signal Process.*, vol. 63, no. 24, pp. 6510–6523, Dec. 2015.
- [31] A. Sandryhaila and J. M. F. Moura, "Discrete signal processing on graphs," *IEEE Trans. Signal Process.*, vol. 61, no. 7, pp. 1644–1656, Apr. 2013.
- [32] A. Sandryhaila and J. M. F. Moura, "Discrete signal processing on graphs: Graph filters," in *Proc. IEEE Int. Conf. Acoust., Speech Signal Process.*, May 2013, pp. 6163–6166.
- [33] A. Sandryhaila and J. M. F. Moura, "Discrete signal processing on graphs: Graph Fourier transform," in *Proc. IEEE Int. Conf. Acoust., Speech Signal Process.*, May 2013, pp. 6167–6170.
- [34] A. Sandryhaila and J. M. F. Moura, "Discrete signal processing on graphs: Frequency analysis," *IEEE Trans. Signal Process.*, vol. 62, no. 12, pp. 3042–3054, Jun. 2014.
- [35] A. V. Oppenheim, A. S. Willsky, and S. H. Nawab, *Signals and Systems* (Prentice-Hall Signal Processing Series). Upper Saddle River, NJ, USA: Prentice-Hall, 1997.
- [36] N. J. Higham, *Functions of Matrices: Theory and Computation* (Other Titles in Applied Mathematics). Philadelphia, PA, USA: Society for Industrial and Applied Mathematics, 2008.
- [37] F. Zhang and E. R. Hancock, "Graph spectral image smoothing using the heat kernel," *Pattern Recognit.*, vol. 41, no. 11, pp. 3328–3342, Nov. 2008.
- [38] D. Thanou, X. Dong, D. Kressner, and P. Frossard, "Learning heat diffusion graphs," *IEEE Trans. Signal Inf. Process. Netw.*, vol. 3, no. 3, pp. 484–499, Sep. 2017.
- [39] M. Benzi and I. Simunec, "Rational Krylov methods for fractional diffusion problems on graphs," *BIT Numer. Math.*, Jul. 2021. [Online]. Available: <https://link.springer.com/article/10.1007/s10543-021-00881-0#citeas>
- [40] M. Ilic, F. Liu, I. Turner, and V. Anh, "Numerical approximation of a fractional-in-space diffusion equation, I," *Fractional Calculus Appl. Anal.*, vol. 8, no. 3, pp. 323–341, 2005.
- [41] A. P. Riascos and J. L. Mateos, "Fractional dynamics on networks: Emergence of anomalous diffusion and Lévy flights," *Phys. Rev. E, Stat. Phys. Plasmas Fluids Relat. Interdiscip. Top.*, vol. 90, no. 3, Sep. 2014, Art. no. 032809.
- [42] E. Estrada, "Path Laplacians versus fractional Laplacians as nonlocal operators on networks," *New J. Phys.*, vol. 23, no. 7, Jul. 2021, Art. no. 073049.
- [43] H. Antil, T. Berry, and J. Harlim, "Fractional diffusion maps," *Appl. Comput. Harmon. Anal.*, vol. 54, pp. 145–175, Sep. 2021.
- [44] A. V. Oppenheim and R. W. Schaffer, *Discrete-Time Signal Processing*, 3rd ed. Essex, U.K.: Pearson Education, 2009.
- [45] V. Välimäki, *Discrete-Time Modeling of Acoustic Tubes Using Fractional Delay Filters*. Espoo, Finland: Helsinki Univ. Technology, 1995.
- [46] National Climatic Data Center. Accessed: Nov. 30, 2021. [Online]. Available: <ftp://ftp.ncdc.noaa.gov/pub/data/gsoad>



GUILHERME B. RIBEIRO was born in Brazil. He received the B.Sc. degree in electronic engineering and the M.Sc. degree in electrical engineering from the Federal University of Pernambuco (UFPE), in 2016 and 2018, respectively, where he is currently pursuing the doctoral degree in graph signal processing. His research interests include geometric algebra, data science, and data visualization.



JOSÉ R. DE OLIVEIRA NETO (Member, IEEE) was born in Brazil. He received the B.Sc., M.Sc., and Ph.D. degrees in electrical engineering from the Federal University of Pernambuco (UFPE), Brazil, in 2013, 2015, and 2019, respectively. He is currently an Assistant Professor with the Department of Mechanical Engineering, UFPE. His main research interests include digital signal processing, embedded systems, and hardware implementations.



JULIANO B. LIMA (Senior Member, IEEE) was born in Brazil. He received the M.Sc. and Ph.D. degrees in electrical engineering from the Federal University of Pernambuco (UFPE), Brazil, in 2004 and 2008, respectively. Since 2015, he has been a Research Productivity Fellow awarded by the Conselho Nacional de Desenvolvimento Científico e Tecnológico. He is currently an Associate Professor with the Department of Electronics and Systems, UFPE. His main research interests

include discrete and number-theoretic transforms, and their applications in digital signal processing, communications, and cryptography.

...